Journal of Sound and Vibration (2001) **247**(2), 261–277
doi:10.1006/jsvi.2001.3729, available online at http://www.idealibrary.com on IDEAL®

THE INFLUENCE OF CENTRIPETAL AND CORIOLIS FORCES ON THE DYNAMIC RESPONSE OF LIGHT BRIDGES UNDER MOVING VEHICLES

G. T. MICHALTSOS

National Technical University of Athens, 42, *Patission str*., *Athens* 10 682, *Greece*.
E-mail: *michalts@central.ntua.gr*

(*Received* 26 *May* 2000, *and in final form* 19 *March* 2001)

This paper deals with the linear dynamic response of a simply supported light (steel) bridge under a moving vehicle of constant magnitude and velocity. This analysis focuses attention on the usually neglected influence of the centripetal force, Coriolis force and vehicle's rotatory inertia. The individual and coupling effects of these forces on the dynamic response of the bridge in connection with the magnitude of the velocity of the moving vehicle are thoroughly discussed. A variety of numerical results allows one to draw important conclusions for structural design purposes.

1. INTRODUCTION

The study and the determination of the influence of dynamic loads on elastic structures is a very old and complicated problem, especially the determination of the dynamic effect of moving loads on elastic structures and particularly on bridges very complex. Many systems in civil engineering, particularly in the design of bridges can be idealized as a flexible beam under a moving mass. The existence of a moving mass, causing non-linearity, makes the problem very difficult.

A number of works have been reported during the last 100 years trying to present reliable solutions for such a multi-parameter problem by using two different methods: The first one is to perform tests and the second is that of pure theoretical investigation. In recent years, transport engineering has experienced serious advances characterized by increasingly higher speeds and weights of vehicles, as a result of which vibrations and dynamic stresses larger than ever before have been developed. From the historical viewpoint, the problem of moving loads was first considered approximately for the case where the mass of the girder was negligible compared to the mass of a single moving load of constant magnitude [1–3]. The other extreme case in which the mass of the moving load was negligible compared to the mass of the girder was originally studied by Krylov [4] and later by Timoshenko [5] and Lowan [6]. The more complicated problem including both the parameters, the load mass and the mass of the girder, was studied by other investigators among whom should be mentioned Steuding [7], Schallemcamp [8] and Bolotin [9]. A very thorough treatise on the dynamic response of several types of railway bridges traversed by steam locomotives was presented by Inglis [10] using harmonic analysis. Interesting analyses were also presented by Hillerborg [11] using Fourier's analysis and by Biggs *et al.* [12] using the Inglis technique. The problem of the dynamic response of bridges under moving loads was reviewed in detail by Timoshenko [13], and later on by Kolousek [14]. The extended

0022-460X/01/420261 + 17 $35.00/0

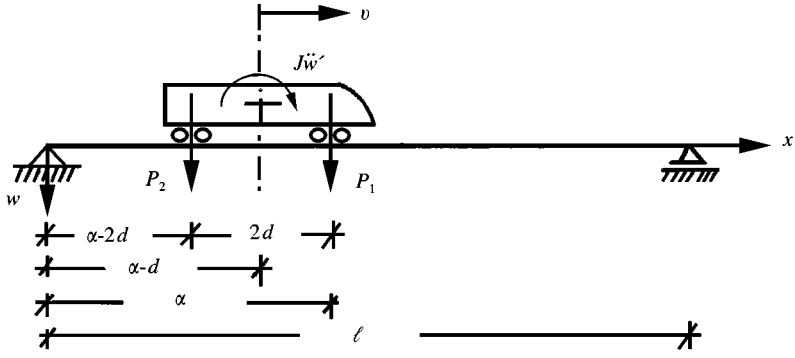

Figure 1. Simply supported uniform beam traversed by a vehicle of mass M with constant velocity v.

review reported by Fryba [15] in his excellent monograph on this subject should also be mentioned. These analyses have been extended to simple frames subjected to moving loads by Karaolides and Kounadis [16] and thereafter to a two-bar frame under a moving load in which the effect of axial motion has been taken into account [17]. Some partial results regarding the effects of the mass of a moving load on the dynamic response of a simply supported beam were recently presented [18].

In all the above studies, the response of laterally vibrating beams and frames due to moving loads was established on the basis of standard dynamic analysis which neglects the effects of both centripetal force, Coriolis force and rotatory inertia, associated with the mass of the moving vehicle which follows the transverse motion of the flexural vibrating beam. A first study of the effect of centripetal and Coriolis forces of a single moving mass on the dynamic response of a light bridge is contained in a paper which has been submitted for publication by Michaltsos and Kounadis [19].

The main goal of this analysis dealing with light simply supported bridges (e.g., made of steel) under heavy moving vehicles is to discuss the conditions under which the above usually secondary effects must be taken into account and also to determine the bridge spans for which it is necessary to use a full model of the vehicles.

2. MATHEMATICAL FORMULATION

Consider the simply supported beam, shown in Figure 1, of length ℓ, having a prismatic cross-section with constant mass per unit length m and flexural rigidity EI, made from linear, homogeneous and isotropic material. Attention is focused on light one-span beams such as bridges made from latticed-steel girders with the above geometric characteristics.

The beam is traversed by a heavy vehicle, shown in Figure 2, having mass M with rotational inertia J moving at constant velocity v. An unfavourable case is a railway locomotive. The position of the vehicle is determined by the distance a of its front wheels from the left of the bridge. Hence, its position α, from the left end of the beam, at any time t is equal to $vt(=a)$, where t is measured from the instant the load enters the span. Before that instant, the deflection throughout the length of the beam is assumed to be zero. One continues by adopting the assumptions of the theory of small vibrations, Navier's hypothesis and Saint Venant's principle. Assuming that the curvature rays $R(a)$ and $R(a-2d)$ are (practically) equal (see Figure 3), it is consequent that only then the perpendicular at point Γon the tangent of the beam-curve passes from point K. Then the

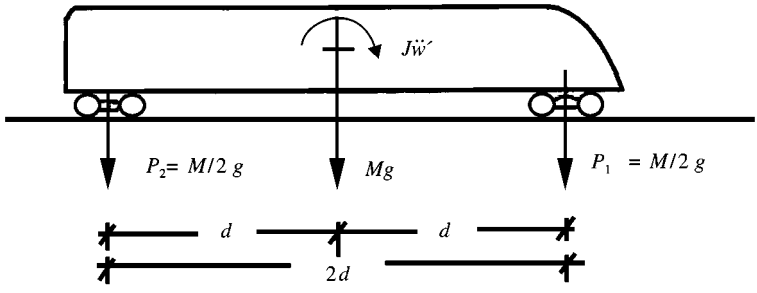

Figure 2. Locomotive (heavy vehicle) of mass M and mass rotatory inertia J.

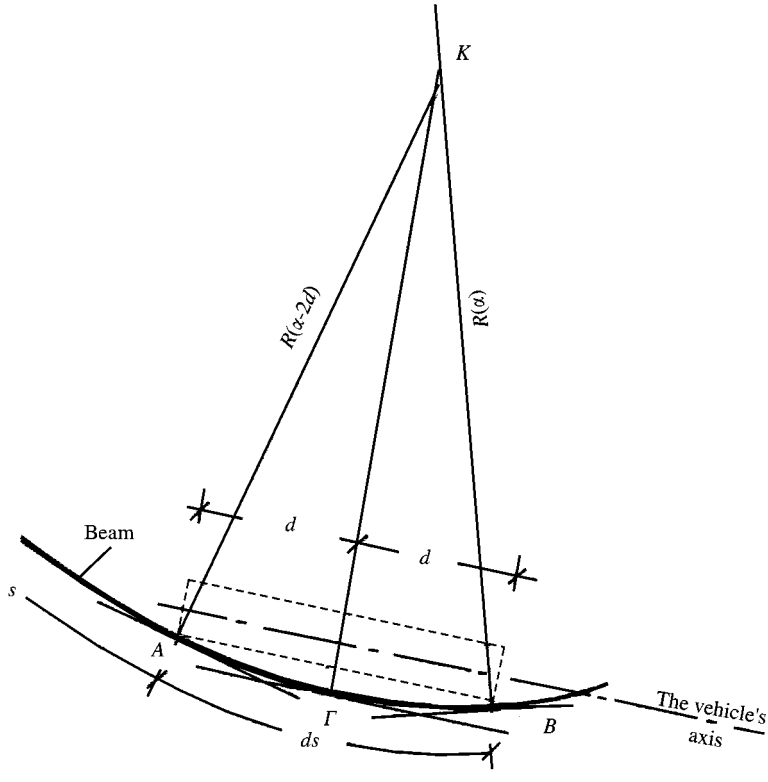

Figure 3. Determination of the new position of the vehicle's axis.

vehicle axis (see Figure 3) is parallel to the above tangent of the beam-curve. Therefore, it is valid that

$$\rho = \varphi = w'(s + \mathrm{d}s) = w'(\alpha - d).$$

Ignoring the changes of the velocity of the vehicle or assuming that the locomotive moves on the bridge with a constant velocity v, one can establish the governing differential equation of motion for a slender beam, after neglecting the effects of longitudinal motion

and damping. Fryba [15] gives this equation using the Dirac function and its derivative:

$$EI\frac{\partial^4 w(x,t)}{\partial x^4}+\left[m+\frac{M}{2}\,\delta(x-\alpha)+\frac{M}{2}\,\delta(x-\alpha+2d)\right]\frac{\partial^2 w(x,t)}{\partial t^2}-J\delta'(x-\alpha+d)\frac{\partial^3 w(x,t)}{\partial x\partial t^2}$$

$$=\frac{M}{2}\,\mathbf{g}\delta(x-\alpha)+\frac{M}{2}\,\mathbf{g}\delta(x-\alpha+2d). \tag{1}$$

Clearly, $P = M\mathbf{g}$, where $\mathbf{g}$ is the gravitational acceleration. The associated boundary and initial conditions are, respectively:

$$w(0,t)=w(\ell,t)=w''(0,t)=w''(\ell,t)=0 \quad \text{and} \quad w(x,0)=\dot{w}(x,0)=0, \tag{2,3}$$

where the prime denotes differentiation with respect to x while the dot to time t.

In contrast to classical dynamic analysis, it is further assumed that the mass M of the load P is not negligible but of comparable magnitude with that of the total mass of the beam $m\ell$. As a consequence, one must include the effects of Coriolis force (complementary acceleration) and of centripetal force (acceleration related to the curvature R of the deflection curve) associated with the mass M of the moving load $P = (M\mathbf{g})$. These forces are given by

$$-M\,(v^2/R)=Mv^2w''(x,t) \quad \text{and} \quad 2Mv\dot{w}'(x,t) \tag{4}$$

where $1/R = -w''(x,t)$

Since both forces have the same direction with the inertia force (per unit length) of the beam, $m\ddot{w}(x,t)$, equation (1) after rearrangement becomes

$$EIw''''(x,t)+m\ddot{w}(x,t)=(M/2)[\mathbf{g}-\ddot{w}(x,t)-v^2w''(x,t)-2v\dot{w}'(x,t)]\delta(x-\alpha)$$

$$+(M/2)[\mathbf{g}-\ddot{w}(x,t)-v^2w''(x,t)-2v\dot{w}'(x,t)]\delta(x-\alpha+2d)$$

$$+J\ddot{w}'(x,t)\delta(x-\alpha+d) \tag{5}$$

where

$$0\leqslant t\leqslant \ell/v.$$

A series solution of equation (5) in terms of normal modes can be sought in the form

$$w(x,t)=\sum_n X_n(x)T_n(t), \tag{6}$$

where $X_n(x)$ is the shape function for the nth mode of the freely vibrating beam, while $T_n(t)$ is the corresponding modal amplitude which has to be determined. Introducing the last expression of $w(x,t)$ into equation (5), one obtains

$$EI\sum_n X_n''''(x)T_n(t)+m\sum_n X_n(x)\ddot{T}_n(t)$$

$$=\frac{M}{2}\left[\mathbf{g}-\sum_n X_n(x)\ddot{T}_n(t)-v^2\sum_n X_n''(x)T_n(t)-2v\sum_n X_n'(x)\dot{T}_n(t)\right]\delta(x-\alpha)$$

$$+\frac{M}{2}\left[\mathbf{g}-\sum_n X_n(x)\ddot{T}_n(t)-v^2\sum_n X_n''(x)T_n(t)-2v\sum_n X_n'(x)\dot{T}_n(t)\right]\delta(x-\alpha+2d)$$

$$+J\sum_n X_n'(x)\ddot{T}_n(t)\delta(x-\alpha+d). \tag{7}$$

The freely vibrating beam is governed by the following equation:

$$EI\sum_n X_n''''(x)T_n(t) - m\sum_n \omega_n^2 X_n(x)T_n(t) = 0, \tag{8}$$

where due to conditions (2) one can write:

$$X_n = \sin n\pi x/\ell, \qquad \omega_n^2 = n^4\pi^4 EI/m\ell^4, \qquad n = 1, 2, \ldots. \tag{9}$$

Introducing equation (8) into equation (7) produces

$$\begin{aligned} &m\sum_n X_n(x)\ddot{T}_n(t) + m\sum_n \omega_n^2 X_n(x)T_n(t) \\ &= \frac{M}{2}\left[\mathbf{g} - \sum_n X_n(x)\ddot{T}_n(t) - v^2\sum_n X_n''(x)T_n(t) - 2v\sum_n X_n'(x)\dot{T}_n(t)\right]\delta(x-\alpha) \\ &\quad + \frac{M}{2}\left[\mathbf{g} - \sum_n X_n(x)\ddot{T}_n(t) - v^2\sum_n X_n''(x)T_n(t) - 2v\sum_n X_n'(x)\dot{T}_n(t)\right]\delta(x-\alpha+2d) \\ &\quad + J\sum_n X'_n(x)\ddot{T}_n(t)\delta(x-\alpha+d) \end{aligned} \tag{10}$$

Multiplication of the last equation by X_k ($k \neq n$) and integrating from 0 to ℓ leads to

$$\begin{aligned} &\ddot{T}_n(t) + \omega_n^2 T_n = (M\mathbf{g}/m\ell)\,X_n(\alpha) \\ &\quad - \frac{M}{m\ell}X_n(\alpha)\left[\sum_{k=1}^{\infty} X_k(\alpha)\ddot{T}_k(t) + v^2\sum_{k=1}^{\infty} X_k''(\alpha)T_k(t) + 2v\sum_{k=1}^{\infty} X_k'(\alpha)\dot{T}_k(t)\right] \\ &\quad + \frac{M\mathbf{g}}{m\ell}X_n(\alpha-2d) - \frac{M}{m\ell}X_n(\alpha-2d)\left[\sum_{k=1}^{\infty} X_k(\alpha-2d)\ddot{T}_k(t) + v^2\sum_{k=1}^{\infty} X_k''(\alpha-2d)T_k(t)\right. \\ &\quad \left. + 2v\sum_{k=1}^{\infty} X_k'(\alpha-2d)\dot{T}_k(t)\right] - \frac{2J}{m\ell}X_n(\alpha-d)\sum_{k=1}^{\infty} X_k''(\alpha-d)\ddot{T}_k(t) \\ &\quad - \frac{2J}{m\ell}X_n'(\alpha-d)\sum_{k=1}^{\infty} X_k'(\alpha-d)\ddot{T}_k(t). \end{aligned} \tag{11}$$

Clearly, a closed-form solution of equation (11) is not possible. However, one can seek approximate solutions. A first approximate solution of equation (11) is obtained by considering as loading, firstly, the force $P = M\mathbf{g}/2$ and secondly the moment m_b. This leads to

$$\begin{aligned} T_n^P(t) &= (M\mathbf{g}/m\ell)\,(1/(\omega_n^2 - \Omega_n^2))\,[\sin\Omega_n t - \Omega_n/\omega_n \sin\omega_n t]. \\ T_n^{mb}(t) &= (m_b/m\ell)(n\pi/\ell)\,(1/(\omega_n^2 - \Omega_n^2))\,[\cos\Omega_n t - \Omega_n/\omega_n \cos\omega_n t], \end{aligned} \tag{12}$$

where

$$\Omega_n = n\pi v/\ell.$$

Introducing the last expression into the right side of equation (11) due to equation (9) produces the result

$$\ddot{T}_n(t) + \omega_n^2 T_n = F_P(t) + F_P(t - 2d/v)\,\mathrm{H}(\mathrm{t} - 2d/v) + F_m(t - d/v)\,\mathrm{H}(t - d/v)$$

where

$$F_P(t) = \frac{M\mathbf{g}}{m\ell}\sin\Omega_n t - \frac{M^2}{(m\ell)^2}\,\mathbf{g}\sin\Omega_n t\left[\sum_{k=1}^{\infty}\frac{\Omega_k^2}{\omega_k^2 - \Omega_k^2}\sin\Omega_k t\left(-\sin\Omega_k t + \frac{\omega_k}{\Omega_k}\sin\omega_k t\right)\right]$$

$$+ \frac{M^2}{(m\ell)^2}\,\mathbf{g}\sin\Omega_n t\left[\sum_{k=1}^{\infty}\frac{v^2(n^2k^2/\ell^2)}{\omega_k^2 - \Omega_k^2}\sin\Omega_k t\left(\sin\Omega_k t - \frac{\omega_k}{\Omega_k}\sin\omega_k t\right)\right]$$

$$- 2\frac{M^2}{(m\ell)^2}\,\mathbf{g}\sin\Omega_n t\left[\sum_{k=1}^{\infty}\frac{v\,(nk/\ell)\,\Omega_k}{\omega_k^2 - \Omega_k^2}\cos\Omega_k t\,(\cos\Omega_k t - \cos\omega_k t)\right],$$

$$F_m(t) = \frac{2J}{m\ell}\sin\Omega_n t\sum_{k=1}^{\infty}\frac{\Omega_k^2}{\omega_k^2 - \Omega_k^2}\frac{k^2\pi^2}{\ell^2}\sin\Omega_k t\left(-\sin\Omega_k t + \frac{\omega_k}{\Omega_k}\sin\omega_k t\right)$$

$$- \frac{2J}{m\ell}\frac{n\pi}{\ell}\cos\Omega_n t\sum_{k=1}^{\infty}\frac{\Omega_k^2}{\omega_k^2 - \Omega_k^2}\frac{k\pi}{\ell}\cos\Omega_k t\left(-\sin\Omega_k t + \frac{\omega_k}{\Omega_k}\sin\omega_k t\right),$$

with

$$\mathrm{H}(t - \alpha) \text{ the Heaviside's function.} \tag{13}$$

The solution of equation (13) using the initial conditions in equation (3) is given by Duhamel's Integral

$$T_n(t) = \frac{1}{\omega_n}\int_0^t F_P(t^*)\sin\omega_n(t - t^*)\,\mathrm{d}t^*$$

$$+ \frac{1}{\omega_n}\left(\int_0^{t_1} F_P(t_1^*)\sin\omega_n(t_1 - t_1^*)\,\mathrm{d}t_1^*\right)\mathrm{H}\left(t_1 - \frac{2d}{v}\right)$$

$$+ \frac{1}{\omega_n}\left(\int_0^{t_2} F_P(t_2^*)\sin\omega_n(t_2 - t_2^*)\,\mathrm{d}t_2^*\right)\mathrm{H}\left(t_2 - \frac{d}{v}\right) \tag{14}$$

with

$$t_1 = t - 2d/v,\ t_2 = t - d/v. \tag{15}$$

Using the dimensionless parameters

$$\xi = \frac{x}{\ell}, \qquad \bar{v} = (2/\pi)\left(\sqrt{m\ell^2/EI}\right)v, \qquad \tau = t/T_1,$$

$$T_1 = (2/\pi)\sqrt{m\ell^4/EI}, \qquad \bar{M} = M/m\ell, \qquad \bar{d} = d/\ell \tag{16}$$

and that for a long vehicle, as shown in Figure 2, $2J/m\ell^2 = \frac{2}{3}\bar{M}\bar{d}^2$ is valid, one can write

$$\Omega_n t = n\pi\bar{v}\tau, \qquad \omega_n t = 2n^2\pi\tau, \qquad \Omega_n = n\pi\bar{v}/T_1,$$

$$\omega_n = 2n^2\pi/T_1, \qquad \mathrm{d}t = T_1\,\mathrm{d}\tau, \qquad \omega_k/\Omega_k = 2k/\bar{v}. \tag{17}$$

Finally, the dimensionless nth mode displacement $\bar{w}_n(\xi, \tau)$ of the beam is given by

$$\bar{w}_n(\xi, \tau) = \frac{\sin(n\pi\xi)}{2n^2} \int_0^\tau \bar{F}_n(\tau^*) \sin[2n^2\pi(\tau - \tau^*)]\, d\tau^*. \tag{18}$$

where

$$\bar{F}_n(\tau) = \bar{F}_{1n}(\tau) + \bar{F}_{2n}(\tau)$$

$$\begin{aligned}
\bar{F}_{1n}(\tau) = {} & \bar{M} \sin(n\pi\bar{v}\tau) \\
& + 2\bar{M}^2 \sum_{k=1}^{\infty} A_k [\sin(n-2k)\pi\bar{v}\tau + \sin(n+2k)\pi\bar{v}\tau] \\
& + 2\bar{M}^2 \sum_{k=1}^{\infty} B_k [\sin(n\bar{v} - k\bar{v} + 2k^2)\pi\tau + \sin(n\bar{v} + k\bar{v} - 2k^2)\pi\tau] \\
& + 2\bar{M}^2 \sum_{k=1}^{\infty} \Gamma_k [\sin(n\bar{v} - k\bar{v} - 2k^2)\pi\tau + \sin(n\bar{v} + k\bar{v} + 2k^2)\pi\tau] \\
& + \bar{M} \sin(n\pi\bar{v}\tau_1) \\
& + 2\bar{M}^2 \sum_{k=1}^{\infty} A_k [\sin(n-2k)\pi\bar{v}\tau_1 + \sin(n+2k)\pi\bar{v}\tau_1] \\
& + 2\bar{M}^2 \sum_{k=1}^{\infty} B_k [\sin(n\bar{v} - k\bar{v} + 2k^2)\pi\tau_1 + \sin(n\bar{v} + k\bar{v} - 2k^2)\pi\tau_1] \\
& + 2\bar{M}^2 \sum_{k=1}^{\infty} \Gamma_k [\sin(n\bar{v} - k\bar{v} - 2k^2)\pi\tau_1 + \sin(n\bar{v} + k\bar{v} + 2k^2)\pi\tau_1],
\end{aligned}$$

$$\begin{aligned}
\bar{F}_{2n}(\tau) = {} & \frac{2\bar{M}\bar{d}^2}{3} \sum_{k=1}^{\infty} (k\pi)^2(-A_k)\{[-\tfrac{1}{2}\sin(n\pi\bar{v}\tau_2) + \tfrac{1}{4}\sin(n-2k)\pi\bar{v}\tau_2 + \tfrac{1}{4}\sin(n+2k)\pi\bar{v}\tau_2] \\
& + \frac{2k}{\bar{v}} [\tfrac{1}{4}\sin(n\bar{v} - k\bar{v} + 2k^2)\pi\tau_2 + \tfrac{1}{4}\sin(n\bar{v} + k\bar{v} - 2k^2)\pi\tau_2 \\
& - \tfrac{1}{4}\sin(n\bar{v} - k\bar{v} - 2k^2)\pi\tau_2 + \tfrac{1}{4}\sin(n\bar{v} + k\bar{v} + 2k^2)\pi\tau_2]\} \\
& - \frac{2\bar{M}\bar{d}^2}{3} \sum_{k=1}^{\infty} (k\pi)^2(-A_k)\{[\tfrac{1}{4}\sin(n-2k)\pi\bar{v}\tau_2 - \tfrac{1}{4}\sin(n+2k)\pi\bar{v}\tau_2] \\
& + \frac{2k}{\bar{v}} [-\tfrac{1}{4}\sin(n\bar{v} + k\bar{v} - 2k^2)\pi\tau_2 + \tfrac{1}{4}\cos(n\bar{v} - k\bar{v} + 2k^2)\pi\tau_2 \\
& - \tfrac{1}{4}\sin(n\bar{v} - k\bar{v} - 2k^2)\pi\tau_2 + \tfrac{1}{4}\cos(n\bar{v} + k\bar{v} + 2k^2)\pi\tau_2]\}
\end{aligned}$$

with

$$A_k = -(\bar{v}^2/(4k^2 - \bar{v}^2)), \qquad B_k = -\bar{v}(2k-1)/8k(2k+1), \qquad \Gamma_k = \bar{v}(2k+1)/8k(2k-1),$$

$$\tau_1 = \tau - 2\bar{d}/\bar{v}, \qquad \tau_2 = \tau - \bar{d}/\bar{v}. \tag{19}$$

TABLE 1

Percentile comparison of dimensionless deflections of the middle of the bridge for cases: (*a*) *of a moving load mass with centripetal and Coriolis forces* (*W*); (*b*) *of a vehicle model without those forces and wheelbase* 2*d* (*WP*); (*c*) *of the above model where centripetal and Coriolis are included* (*WC*) *and* (*d*) *of model* (*c*) *including, in addition, the effect of rotatory inertia* (*WCM*)

	$2\bar{d}$	0·10					0·20				
$\bar{M}$	$\bar{v}$	0·10	0·20	0·30	0·40	0·50	0·10	0·20	0·30	0·40	0·50
0·10	W	0·0163	0·0166	0·0179	0·0163	0·0196	0·0163	0·0166	0·0179	0·0163	0·0196
	WP	0·0166	0·0160	0·0175	0·0162	0·0194	0·0160	0·0168	0·0158	0·0158	0·0170
	WC	0·0161	0·0161	0·0173	0·0161	0·0191	0·0155	0·0163	0·0155	0·0158	0·0170
	WCM	0·0162	0·0161	0·0172	0·0160	0·0190	0·0152	0·0167	0·0158	0·0162	0·0166
	D_1	−0·49	−0·19	0·52	0·44	0·42	2·37	−2·21	−1·46	−2·53	2·47
	D_2	2·65	−0·37	1·86	1·50	2·05	5·53	0·60	0·06	−2·53	2·41
	D_3	0·80	3·34	4·18	2·18	2·94	7·76	−0·24	13·48	0·92	17·92
0·20	W	0·0348	0·0337	0·0340	0·0324	0·0379	0·0348	0·0337	0·0340	0·0324	0·0379
	WP	0·0332	0·0322	0·0352	0·0325	0·0390	0·0320	0·0336	0·0315	0·0314	0·0343
	WC	0·0323	0·0323	0·0343	0·0319	0·0378	0·0308	0·0317	0·0308	0·0314	0·0344
	WCM	0·0320	0·0323	0·0342	0·0318	0·0377	0·0312	0·0325	0·0311	0·0323	0·0336
	D_1	0·72	0·12	0·40	0·31	0·42	−1·25	−2·27	−0·90	−2·75	2·50
	D_2	3·58	−0·22	2·95	2·19	3·45	2·53	3·47	1·22	−2·87	2·29
	D_3	8·79	4·27	−0·67	1·89	0·58	11·48	3·69	9·35	0·12	12·85
0·30	W	0·0554	0·0537	0·0518	0·0527	0·0572	0·0554	0·0537	0·0518	0·0527	0·0572
	WP	0·0500	0·0485	0·0532	0·0487	0·0589	0·0481	0·0505	0·0470	0·0471	0·0520
	WC	0·0500	0·0489	0·0512	0·0475	0·0563	0·0477	0·0463	0·0472	0·0470	0·0522
	WCM	0·0496	0·0488	0·0510	0·0473	0·0560	0·0488	0·0474	0·0471	0·0485	0·0509
	D_1	0·64	0·10	0·45	0·27	0·48	−2·29	−2·30	0·34	−3·03	2·51
	D_2	0·78	−0·70	4·31	3·00	5·21	−1·57	6·43	−0·08	−2·90	2·22
	D_3	11·69	9·91	1·59	11·36	2·07	13·55	13·15	9·93	8·67	12·29
0·40	W	0·0783	0·0761	0·0726	0·0758	0·0805	0·0783	0·0761	0·0726	0·0758	0·0805
	WP	0·0667	0·0649	0·0713	0·0649	0·0790	0·0641	0·0674	0·0625	0·0626	0·0702
	WC	0·0687	0·0654	0·0678	0·0640	0·0746	0·0653	0·0631	0·0647	0·0631	0·0701
	WCM	0·0684	0·0653	0·0674	0·0643	0·0742	0·0664	0·0632	0·0644	0·0649	0·0684
	D_1	0·41	0·14	0·52	−0·42	0·59	−1·65	−0·21	0·42	−2·77	2·48
	D_2	−2·54	−0·66	5·72	1·03	6·40	−3·42	6·53	−2·85	−3·62	2·63
	D_3	14·44	16·50	7·66	17·90	8·43	17·95	20·29	12·72	16·65	17·57
0·50	W	0·1032	0·1007	0·0961	0·1016	0·1073	0·1032	0·1007	0·0961	0·1016	0·1073
	WP	0·0834	0·0813	0·0895	0·0811	0·0993	0·0802	0·0842	0·0779	0·0780	0·0881
	WC	0·0883	0·0824	0·0841	0·0822	0·0931	0·0844	0·0809	0·0832	0·0792	0·0889
	WCM	0·0879	0·0824	0·0837	0·0825	0·0925	0·0840	0·0810	0·0824	0·0816	0·0867
	D_1	0·39	0·07	0·53	−0·37	0·59	0·52	−0·08	0·93	−2·92	2·55
	D_2	−5·11	−1·27	6·96	−1·72	7·35	−4·49	4·01	−5·44	−4·40	1·69
	D_3	17·35	22·23	14·84	23·04	15·95	22·91	24·33	16·61	24·48	23·74

3. NUMERICAL RESULTS AND DISCUSSION

In this section, numerical results are presented in both graphical and tabular forms. The individual and coupling effects on the dynamic response of centripetal and Coriolis forces combined with various parameters, such as vehiclemass, distance of wheel axles (wheelbase) and velocity of the moving vehicle are discussed in detail.

The mathematical model discussed herein is related to a real bridge with a span of $\sim$100 m, weight per unit length of $\sim$40 kN/m and moment of inertia $I = \sim 1{\cdot}50\ \mathrm{m}^4$, which

TABLE 2

Percentile comparison of dimensionless deflections of the middle of the bridge for cases: (*a*) *of a moving load mass with centripetal and Coriolis forces* (*W*); (*b*) *of a vehicle model without those forces and wheelbase* 2*d* (*WP*); (*c*) *of the above model where centripetal and Coriolis forces are included* (*WC*) *and* (*d*) *of model* (*c*) *including, in addition, the effect of rotatory inertia* (*WCM*)

	$2\bar{d}$	0·30					0·40				
$\bar{M}$	$\bar{v}$	0·10	0·20	0·30	0·40	0·50	0·10	0·20	0·30	0·40	0·50
0·10	W	0·0163	0·0166	0·0179	0·0163	0·0196	0·0163	0·0166	0·0179	0·0163	0·0196
	WP	0·0149	0·0144	0·0157	0·0170	0·0157	0·0133	0·0143	0·0136	0·0166	0·0162
	WC	0·0145	0·0145	0·0155	0·0167	0·0155	0·0129	0·0140	0·0136	0·0162	0·0158
	WCM	0·0154	0·0152	0·0160	0·0175	0·0158	0·0144	0·0140	0·0146	0·0178	0·0168
	D_1	−5·93	−4·66	−3·05	−4·95	−1·52	−10·37	−0·21	−6·78	−8·96	−5·99
	D_2	−3·23	−5·25	−1·80	−3·01	−0·44	−8·02	2·35	−6·50	−6·55	−3·80
	D_3	5·74	9·52	11·57	−6·87	23·88	13·28	18·80	22·72	−8·23	16·31
0·20	W	0·0348	0·0337	0·0340	0·0324	0·0379	0·0348	0·0337	0·0340	0·0324	0·0379
	WP	0·0299	0·0291	0·0319	0·0339	0·0315	0·0271	0·0287	0·0275	0·0334	0·0323
	WC	0·0286	0·0295	0·0304	0·0325	0·0308	0·0257	0·0273	0·0274	0·0318	0·0307
	WCM	0·0304	0·0310	0·0315	0·0344	0·0312	0·0295	0·0281	0·0294	0·0351	0·0330
	D_1	−6·82	−4·98	−3·46	−5·43	−1·09	−12·75	−2·94	−6·89	−9·32	−6·84
	D_2	−1·94	−6·24	1·39	−1·42	0·92	−8·05	2·13	−6·48	−4·84	−2·04
	D_3	14·36	8·46	7·99	−5·89	21·45	17·96	19·62	15·15	−7·63	14·80
0·30	W	0·0554	0·0537	0·0518	0·0527	0·0572	0·0554	0·0537	0·0518	0·0527	0·0572
	WP	0·0449	0·0442	0·0478	0·0507	0·0472	0·0407	0·4315	0·0417	0·0501	0·0483
	WC	0·0441	0·0450	0·0444	0·0476	0·0465	0·0392	0·0399	0·0413	0·0466	0·0447
	WCM	0·0449	0·0475	0·0460	0·0506	0·0459	0·0453	0·0428	0·0444	0·0516	0·0485
	D_1	−1·71	−5·27	−3·47	−5·86	1·13	−13·28	−6·70	−6·82	−9·77	−7·88
	D_2	0·13	−7·10	3·97	0·22	2·73	−10·02	0·79	−6·06	−2·94	−0·56
	D_3	23·56	12·83	12·48	4·18	24·40	22·46	25·43	16·66	2·09	17·74
0·40	W	0·0783	0·0761	0·0726	0·0758	0·0805	0·0783	0·0761	0·0726	0·0758	0·0805
	WP	0·0598	0·0594	0·0638	0·0673	0·0630	0·0543	0·0575	0·0561	0·0669	0·0641
	WC	0·0605	0·0608	0·0577	0·0619	0·0630	0·0538	0·0519	0·0555	0·0606	0·0579
	WCM	0·0594	0·0629	0·0600	0·0660	0·0606	0·0616	0·0575	0·0594	0·0675	0·0635
	D_1	1·88	−3·43	−3·88	−6·27	4·04	−12·66	−9·75	−6·67	−10·19	−8·83
	D_2	0·76	−5·62	6·43	2·01	3·96	−11·96	−0·03	−6·64	−0·95	1·05
	D_3	31·87	20·86	20·98	14·78	32·85	27·03	32·29	22·08	12·18	26·76
0·50	W	0·1032	0·1007	0·0961	0·1016	0·1073	0·1032	0·1007	0·0961	0·1016	0·1073
	WP	0·0749	0·0752	0·0797	0·0838	0·0787	0·0679	0·0718	0·0708	0·0835	0·0799
	WC	0·0778	0·0776	0·0731	0·0765	0·0806	0·0691	0·0659	0·0697	0·0740	0·0703
	WCM	0·0745	0·0819	0·0768	0·0821	0·0763	0·0787	0·0734	0·0750	0·0827	0·0778
	D_1	4·38	−5·16	−4·88	−6·83	5·68	−12·17	−10·19	−7·06	−10·52	−9·64
	D_2	0·58	−8·10	3·81	2·12	3·23	−13·74	−2·17	−5·62	0·94	2·70
	D_3	38·49	23·01	25·14	23·71	40·62	31·15	37·14	28·17	22·79	37·93

is traversed by a moving load with velocities $v = 50$, 100, 150, 200 and 250 km/h or in dimensionless form velocities $\bar{v} = 0{\cdot}10$, 0·20, 0·30, 0·40, 0·50 respectively. The velocities are combined with the dimensionless values of vehicle masses $\bar{M} = 0{\cdot}10$, 0·20, 0·30, 0·40, and 0·50 and the dimensionless wheelbases $2\bar{d} = 0{\cdot}10$, 0·20, 0·30 and 0·40.

Numerical results are given in Tables 1 and 2 in which W are the dimensionless deflections of the middle of the bridge, including the effect of centripetal and Coriolis forces,

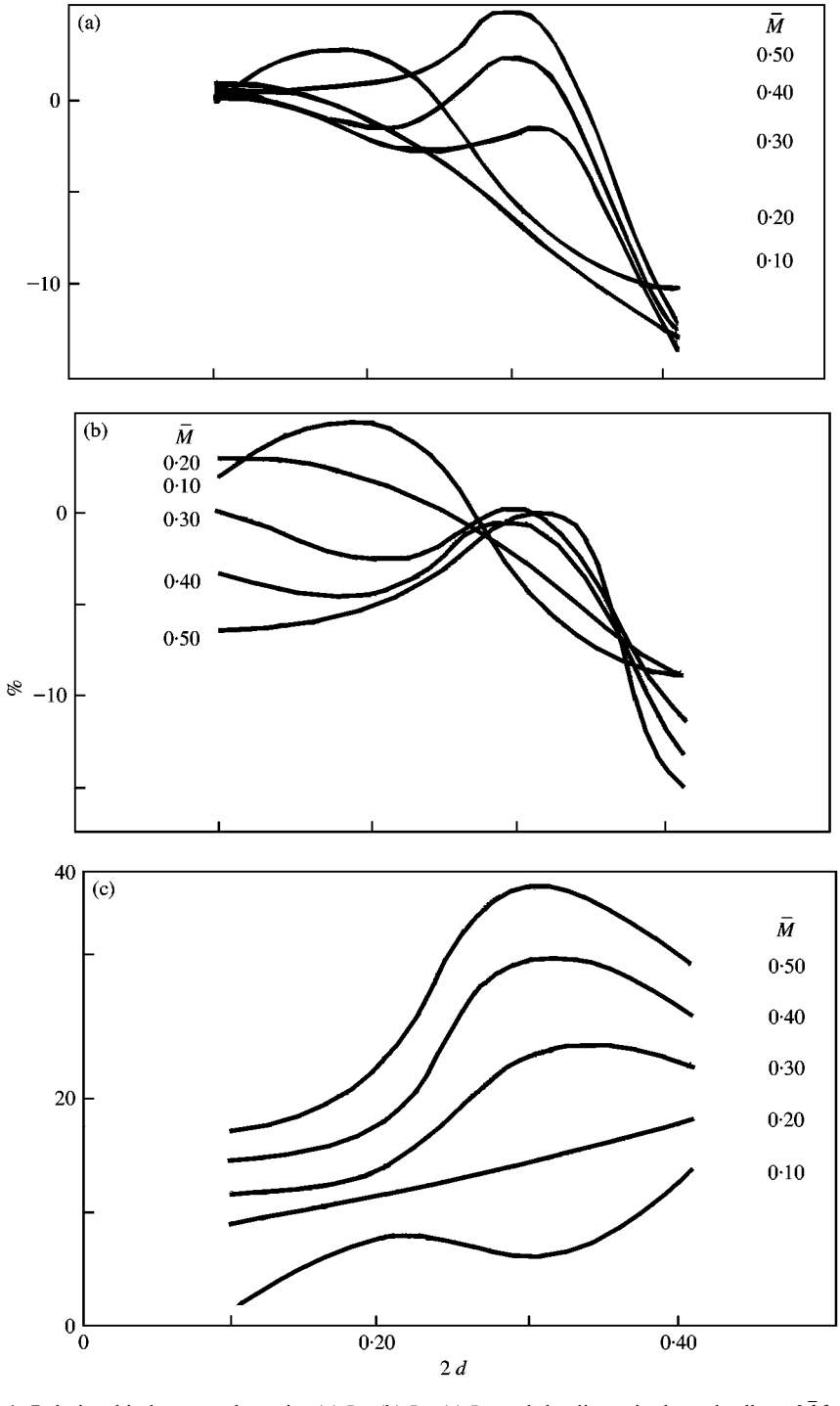

Figure 4. Relationship between the ratios (a) D_1, (b) D_2, (c) D_3 and the dimensionless wheelbase $2\bar{d}$ for various values of the dimensionless mass $\bar{M}$ and dimensionless velocity $\bar{v} = 0{\cdot}10$.

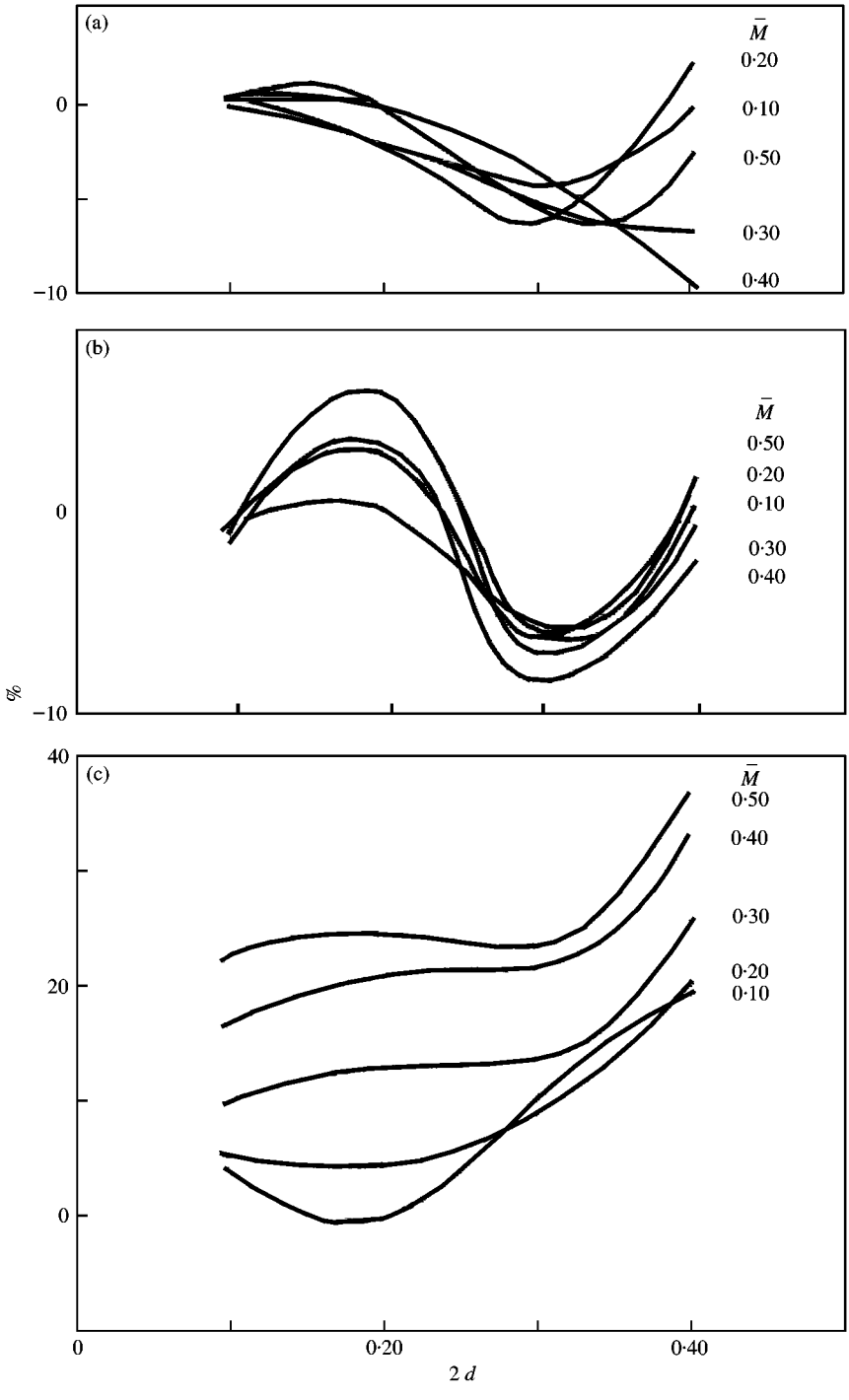

Figure 5. Relationship between the ratios (a) D_1, (b) D_2, (c) D_3 and the dimensionless wheelbase $2\bar{d}$ for various values of the dimensionless mass $\bar{M}$ and dimensionless velocity $\bar{v} = 0{\cdot}20$.

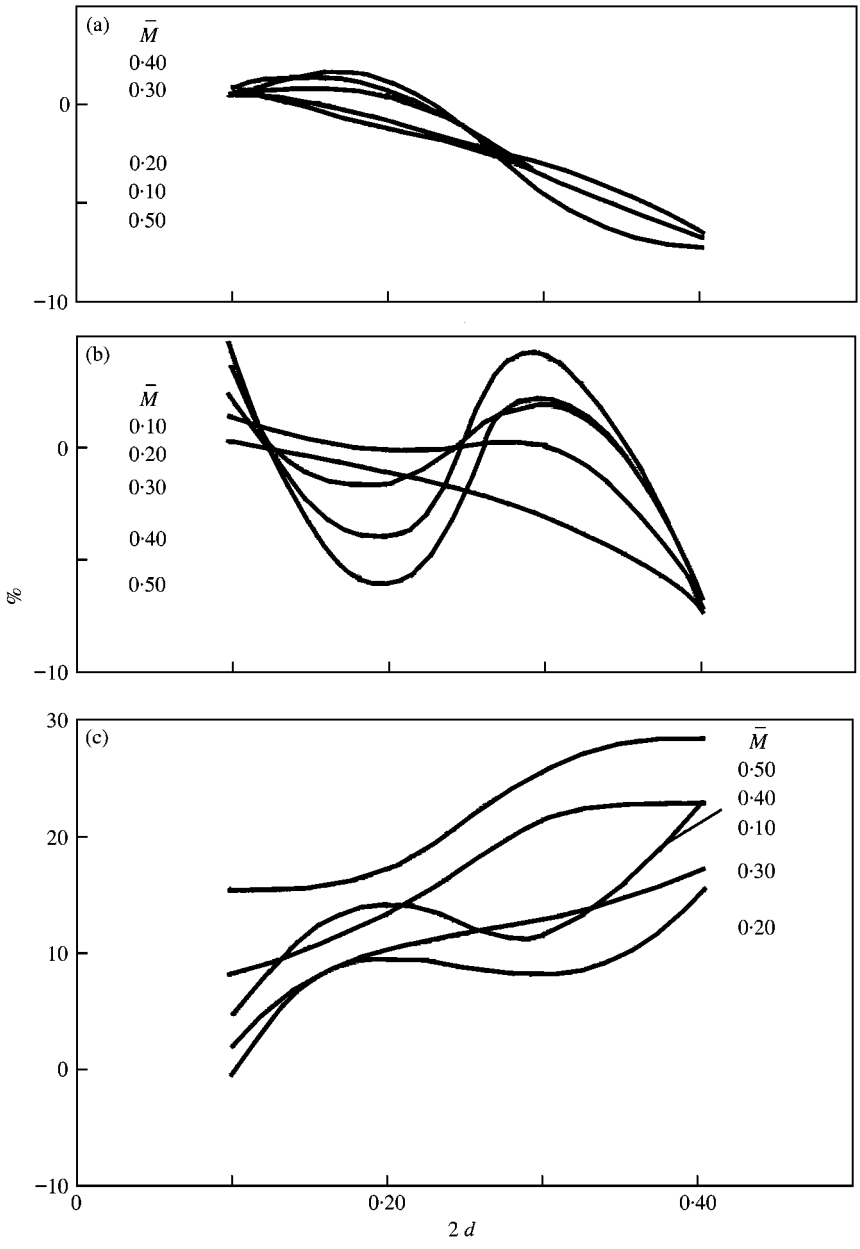

Figure 6. Relationship between the ratios (a) D_1, (b) D_2, (c) D_3 and the dimensionless wheelbase $2\bar{d}$ for various values of the dimensionless mass $\bar{M}$ and dimensionless velocity $\bar{v} = 0{\cdot}30$.

for a moving load mass $\bar{M}$; WP are the dimensionless deflections of the middle of the bridge for a vehicle model with dimensionless mass $\bar{M}$ and dimensionless wheelbase $2\bar{d}$, in which the effects of centripetal and Coriolis forces are neglected; WC are the dimensionless deflections of the above vehicle model, in which the effects of centripetal and Coriolis forces are included; WCM are the dimensionless deflections of the above vehicle model, in which except for the effect of centripetal and Coriolis forces the effect of the vehicle·s mass rotatory

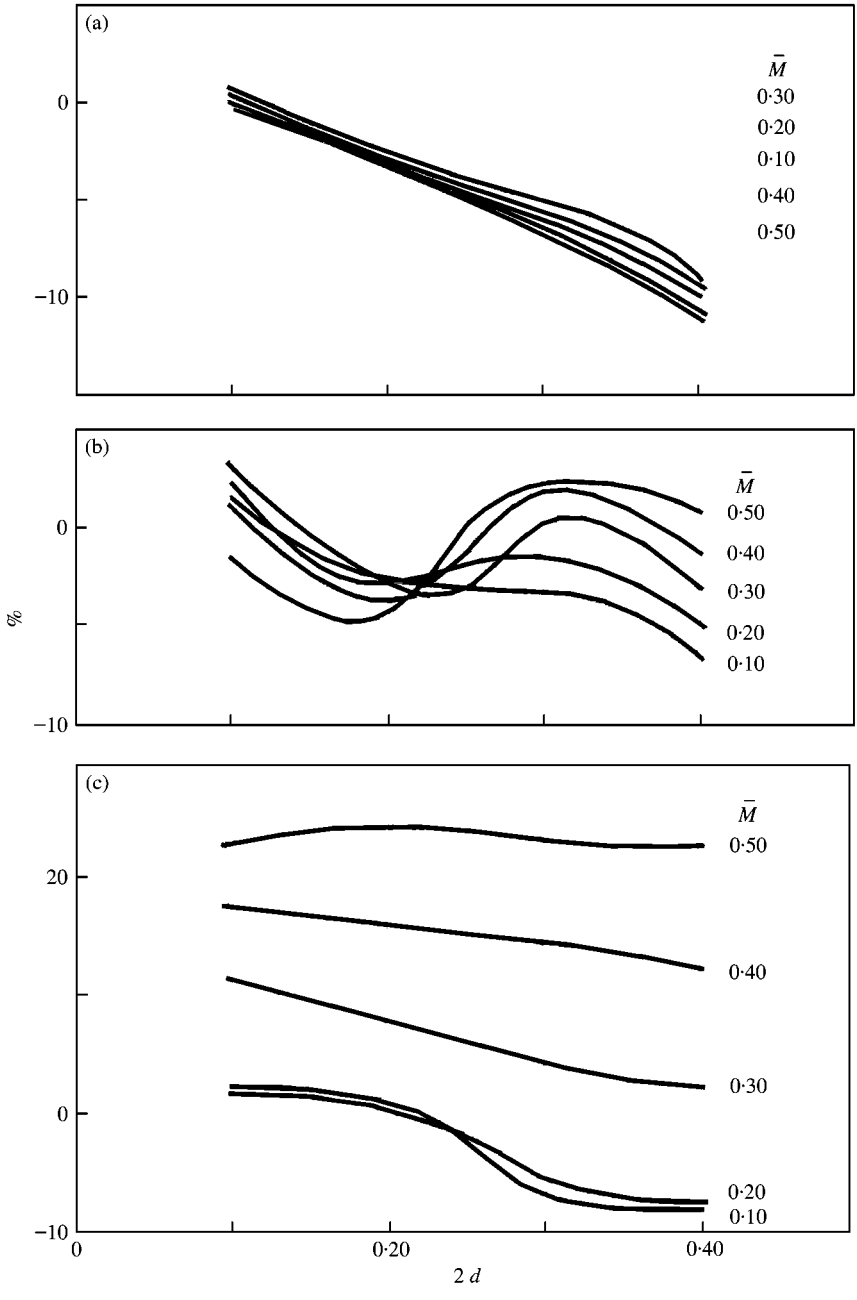

Figure 7. Relationship between the ratios (a) D_1, (b) D_2, (c) D_3 and the dimensionless wheelbase $2\bar{d}$ for various values of the dimensionless mass $\bar{M}$ and dimensionless velocity $\bar{v} = 0{\cdot}40$.

inertia is also included. This last model is considered (for the present paper) as the real vehicle's model. The above deflections concern the middle of the bridge (*at* $\xi = 0{\cdot}5$).

From the plots of Figures 4–8 one can see graphically the relationship between the dimensionless wheelbases $2\bar{d}$ and the deflection ratios $D_1 = (\mathrm{WC} - \mathrm{WCM})/\mathrm{WCM}$ %, $D_2 = (\mathrm{WP} - \mathrm{WCM})/\mathrm{WCM}\%$, $D_3 = (\mathrm{W} - \mathrm{WCM})/\mathrm{WCM}\%$, in connection with the dimensionless vehicle masses $\bar{M}$.

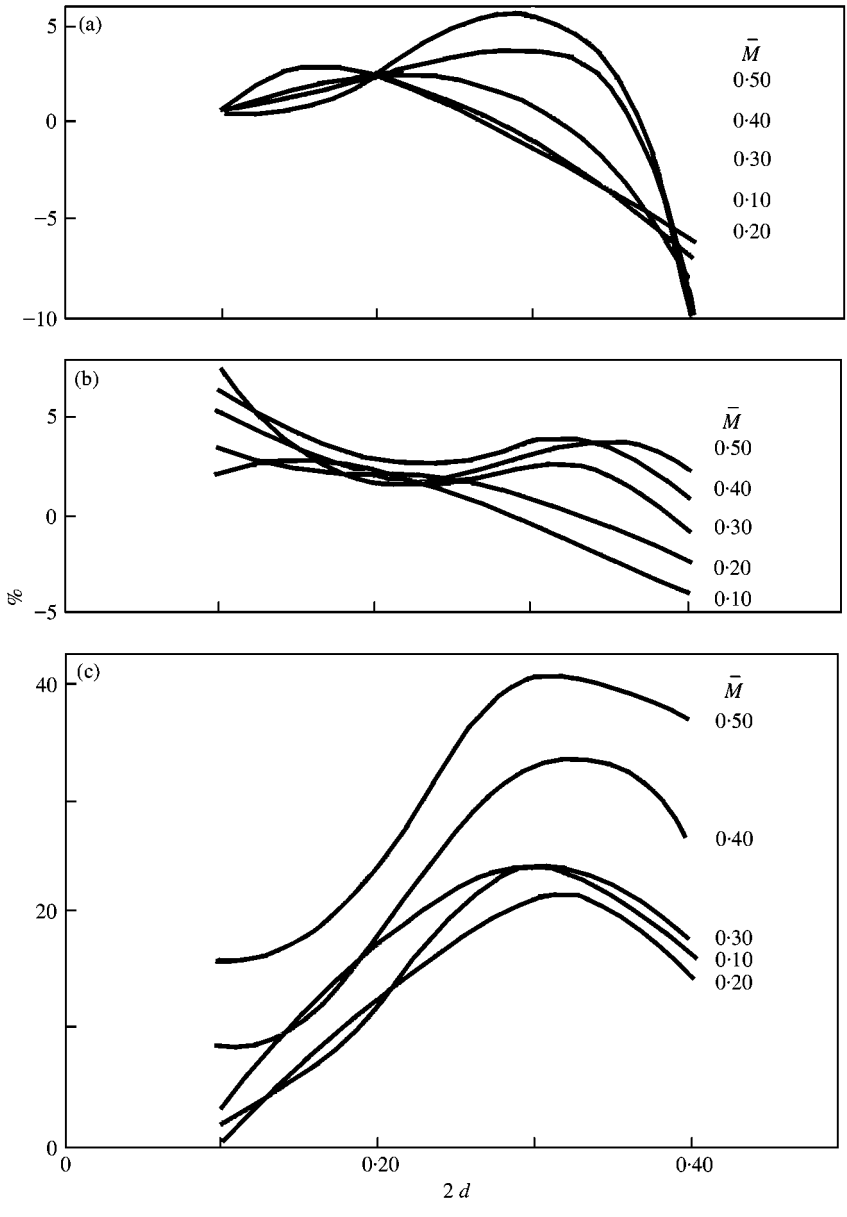

Figure 8. Relationship between the ratios (a) D_1, (b) D_2, (c) D_3 and the dimensionless wheelbase $2\bar{d}$ for various values of the dimensionless mass $\bar{M}$ and dimensionless velocity $\bar{v} = 0{\cdot}50$.

From the above plots, one can easily deduce the following results:

(1) The model of the single-mass load is accurate for values up to $\bar{M} = 0{\cdot}20$. For higher values of $\bar{M}$ (even if the speeds are low) the differences from the real model are higher than 10% and can amount from 25 to 40% (see ratio D_3).
(2) The model of a vehicle with two axes and mass $\bar{M}$ is more accurate than the above model of a one-mass load $\bar{M}$. In this two-axis model, the influences of centripetal and Coriolis forces are neglected. The differences from the exact model are high for low

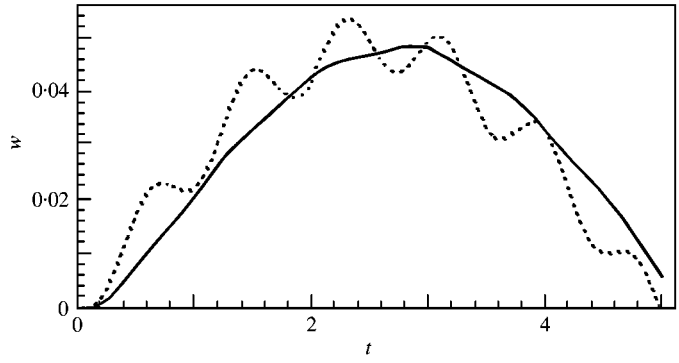

Figure 9. Middle-span deflections of the beam for: $\bar{M} = 0{\cdot}30$, $\bar{v} = 0{\cdot}20$, $2\bar{d} = 0{\cdot}10$. W, ·····; WP, – – – –; WC, ------; WCM, ——.

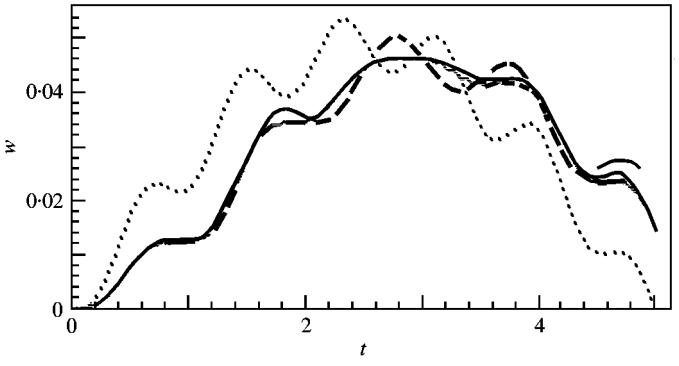

Figure 10. Middle-span deflections of the beam for: $\bar{M} = 0{\cdot}30$, $\bar{v} = 0{\cdot}20$, $2\bar{d} = 0{\cdot}20$. W, ·····; WP, – – – –; WC, ------; WCM, ——.

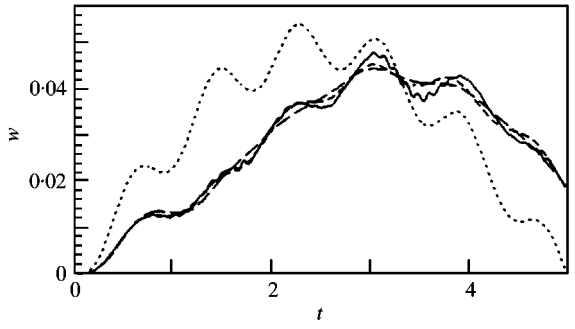

Figure 11. Middle-span deflections of the beam for: $\bar{M} = 0{\cdot}30$, $\bar{v} = 0{\cdot}20$, $2\bar{d} = 0{\cdot}30$. W, ·····; WP, – – – –; WC, ------; WCM, ——.

speeds (independently of the value of wheelbase) amounting from about -8 to 15%, but are low for higher speeds and masses amounting from about -4 to 5%.

(3) The third model which neglects only the vehicle's mass rotatory inertia is more accurate than the others for low values of wheelbase (up to $2\bar{d} = 0{\cdot}20$) independent of speed and magnitude of mass. For wheelbases with values higher than $2\bar{d} = 0{\cdot}20$, the influence of the neglected parameter J becomes very significant and then the differences from the deflections of the real model are from about 10 to 15%.

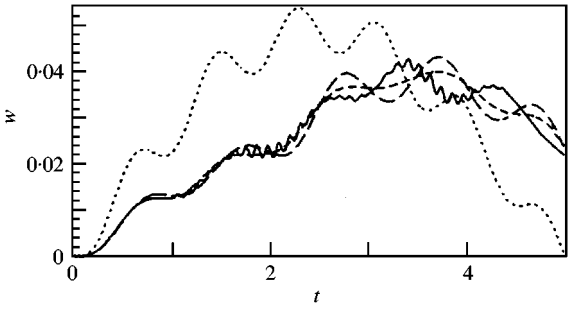

Figure 12. Middle-span deflections of the beam for: $\bar{M} = 0{\cdot}30$, $\bar{v} = 0{\cdot}20$, $2\bar{d} = 0{\cdot}40$. W, ·····; WP, – – – –; WC, ------; WCM, ——.

One can also see (indicatively) in Figures 9–12 the variation of mid-span deflections $\bar{w}(0{\cdot}5, \tau)$ for $\bar{M} = 0{\cdot}30$, $\bar{v} = 0{\cdot}20$ and various dimensionless wheelbases $2\bar{d} = 0{\cdot}10$, $0{\cdot}20$, $0{\cdot}30$ and $0{\cdot}40$. The above four models are presented in the following way: W (pointed lines), WP (long-dashed lines), WC (short-dashed lines) and WCM (continuous lines).

4. CONCLUSIONS

On the basis of the model chosen, one may draw the following conclusions:

1. The effect of centripetal and Coriolis forces is significant for a moving vehicle.
2. The model of the single-mass load can be used only for values of the wheelbase lower than $2\bar{d} = 0{\cdot}10$.
3. The influence of the vehicle's mass rotatory inertia together with the influence of centripetal and Coriolis forces has to be taken into account for values of wheelbase higher than $2\bar{d} = 0{\cdot}10$.

REFERENCES

1. R. WILLIS *et al.* 1849 Preliminary essay to the appendix B: experiments for determining the effects produced by causing weights to travel over bars with different velocities. in *Report of the Commissioners Appointed to Inquire into the Application of Iron to Railway Structures* (G. GREY *et al.*, editors), London: W. Clowes and Sons. [Reprinted in: P. BARLOW 1851 *Journal of Cast Iron and Malleable Iron.* Treatise on the strength of timber.]
2. G. STOKES 1849 *Transactions of Cambridge Philosophical Society Part* 5 707–735. Discussion of a differential equation relating to the breaking of railway bridges. (Reprinted in Mathematical and Physical Papers, 1883, 178–220.)
3. H. ZIMMERMANN 1896 *Centralblatt der Bauverwaltung* **16,** 249–251, 257–260, 264–266, 288. Die Schwingungen eines Tragers mit bewegter Lasts.
4. A. N. KRYLOV 1905 *Mathematical Collection of Papers of the Academy of Sciences*, (A. N. KRILOFF, editor) Vol. 61. Peterburg: Matematischeskii sbornik Akademii Nauk. Uber die erzwungenen Schwingungen von gleichformigen elastischen Staben. Mathematische Annalen.
5. S. P. TIMOSHENKO 1908 *Izvestiya Kievskogo politekhnicheskogo instituta.* Forced vibration of prismatic bars (in Russian). (Also in German: 1911, *Zeitschrift. fuer. Mathematik und Physik* **59**, 163–203, Erzwungene Schwingungen prismatischer Stabe.)
6. A. N. LOWAN 1935 *Philosophical Magazine*, *Series* 7 **19,** 708–715. On transverse oscillations of beams under the action of moving variable loads.
7. H. STEUDING 1934 *Ingenieur-Archiv* 275–305, 265-270. Die Schwingungen von tragern bei bewegten lasten. I, II.

8. A. SCHALLENKAMP 1937 *Ingenieur-Archiv* **8**, 182–198. Schwingungen von tragern bei bewegten lasten.
9. V. V. BOLOTIN 1961. *Izvestiya AN SSSR, Mekhanika I Mashinostroenie* **4**, 109–115. Problem of bridge vibration under the action of a moving load (in Russian).
10. C. E. INGLIS 1934 *A Mathematical Treatise on Vibration in Railway Bridges*. Cambridge: The University Press.
11. A. HILLERBORG 1951 *Kungl. Tekn. Hogskolan, Stockholm*. Dynamic influences of smoothly running loads on simply loads on simply supported girders.
12. J. M. BIGGS, H. S. SUER and J. M. LOUW 1959 *Transactions of the American Society of Civil Engineers* **124**, 291–318. Vibration on simple-span highway bridges.
13. S. P. TIMOSHENKO 1953 *History of the Strength of Materials*. New York: D. van Nostrand Co.
14. V. KOLOUSEK 1956, 1961, 1967 *Dynamics of civil engineering structures. Part I-General problems, second edition*; *Part II-Continuous beams and frame systems, second edition*; *Part III-Selected topics* (in Czech). Prague: SNTL.
15. L. FRYBA 1972 *Vibration of Solids and Structures Under Moving Loads*. Prague: Research Institute of Transport.
16. CH. KARAOLIDES and A. N. KOUNADIS 1983 *Journal of Sound and Vibration* **88**, 37–45. Forced motion of a simple frame subjected to a moving force.
17. D. S. SOPHIANOPOULOS and A. N. KOUNADIS 1989 *Acta Mechanica* **79**, 277–294. The axial motion effect on the dynamic response of a laterally vibrating frame subject to a moving load.
18. G. T. MICHALTSOS, D. SOPHIANOPOULOS and A. N. KOUNADIS 1996 *Journal of Sound and Vibration* **191**, 357–362. The effect of a moving mass and other parameters on the dynamic response of a simply supported beam.
19. G. T. MICHALTSOS and A. N. KOUNADIS 2001 *Journal of Vibration and Control* **7**, 315–326. The effects of centripetal and Coriolis forces on the dynamic response of light bridges under moving loads.